Analytical Methods

ROYAL SOCIETY OF CHEMISTRY

PAPER

View Article Online
View Journal | View Issue

Cite this: *Anal. Methods*, 2024, **16**, 2921

A simplified lateral flow immunosensor for the assay of carcinoembryonic antigen in low-resource settings†

Ioanna Tsogka, Electra Mermiga, Varvara Pagkali, Christos Kokkinos and Anastasios Economou *

Carcinoembryonic antigen (CEA) is a glycoprotein widely used as a tumor marker. In this work, a colorimetric lateral flow immunosensor is developed for rapid and low-cost quantification of CEA in human blood serum. The immunosensor consists of a glass fiber sample/conjugation pad, a nitrocellulose detection pad and a cellulose absorption pad. The detection is based on a sandwich immunoreaction: the sample/conjugation pad is modified with gold nanoparticles (GNPs)-labeled anti-CEA conjugate probes which bind to the CEA target molecules in the sample and the complexes are captured at capture anti-CEA immobilized at the test line. The color intensity of the test line, measured from a scanned image of the strip, is related to the CEA concentration in the sample. The different assay parameters are studied in detail. The linearity holds from 1.25 to 640 ng mL^{-1} of CEA, the instrumental and visual limits of detection are 0.45 and 0.63 ng mL^{-1}, respectively, and the total assay time is 15 min. The specificity of the immunoassay *versus* other cancer biomarkers is satisfactory. The recovery in samples of human serum spiked with CEA is in the range of 81–118% and the coefficient of variation of the method is ≤10%. Results obtained with the lateral flow immunosensor correlated well with a reference radioimmunoassay method (R^2 = 0.99). This immunosensor can be readily applied to CEA monitoring at the point-of-care (POC) or in resource-limited settings thanks to its low-cost and simplicity.

Received 29th February 2024
Accepted 19th April 2024

DOI: 10.1039/d4ay00381k

rsc.li/methods

1 Introduction

Despite the significant advances made in the medical field in recent years, cancer remains one of the world's biggest and most pressing health problems. According to the World Health Organization (WHO), cancer is the second leading cause of death after cardiovascular diseases, accounting for nearly 10 million deaths every year globally (or nearly one in six deaths).[1] 20.3 million new cancer cases and 13.2 million deaths due to cancer are predicted for the year 2030 (ref. 2) while by the end of 2023, a grand total of 1 261 990 cancer deaths are predicted in the European Union alone.[3] The monitoring of tumor biomarkers has been used for a long time in cancer diagnostics as a tool for early clinical detection, prognosis, checking of recurrence and evaluating the response to therapy.[4–6] Carcinoembryonic antigen (CEA) is a glycoprotein involved in cell adhesion and is a universally acknowledged cancer marker (mainly for colorectal, breast, lung and pancreatic cancer).[7–9] The conventional cut-off value for CEA is set to 5 ng mL^{-1}.[10,11] Since CEA exists in many types of normal epithelial cells, it is present, albeit at low levels (<5 ng mL^{-1}), in the blood of healthy adults. However, high blood serum levels of CEA (>15–20 ng mL^{-1}) are associated with a plethora of carcinomas. Thus, the quantification of CEA enables early diagnosis, assessment and monitoring the recurrence the disease.

Among the methods used for CEA detection and quantification in human serum, those based on liquid chromatography-mass spectrometry provide low limits of detection and exceptional selectivity but require expensive and bulky instrumentation as well as laboratory facilities.[12] In addition, a variety of immunoassays have been developed for detecting CEA in serum, such as radioimmunoassays (RIAs), enzyme-linked immunosorbent assays (ELISA), fluorescence immunoassays, chemiluminescence immunoassays, electrochemical immunoassays and surface-enhanced Raman scattering immunoassays.[13–23] However, these assays normally require multiple reagents and several washing steps that increase the complexity of the analytical procedure and the time of the analysis while many of them demand trained personnel, laboratory facilities and complex instrumentation.

On the other hand, lateral flow immunoassays operate on a simplified protocol in which the sample migrates along a strip and the target antigen undergoes an immunoreaction at a narrow test zone modified with a capture antibody, resulting in an analytical signal.[24–28] This operational principle has many

Department of Chemistry, National and Kapodistrian University of Athens, Panepistimiopolis 157 71, Greece. E-mail: aeconomo@chem.uoa.gr

† Electronic supplementary information (ESI) available. See DOI: https://doi.org/10.1039/d4ay00381k

advantages in terms of the operational characteristics and the analytical features of the assay. Lateral flow immunoassays do not require washing steps or addition of reagents, as they rely on unidirectional spontaneous flow of the sample and on reagents immobilized on the strip. The strips are cost-effective because only minute quantities of expensive biorecognition agents are used while the dry reagents are less prone to deactivation so that these devices have relatively long shelf life in ambient conditions. The assay robustness is usually further ensured by incorporating an internal quality control in the form of a control line. The tight spatial confinement of the biorecognition elements at the narrow test zone on the strip induces a high degree of aggregation of the target species at the test zone leading to high detection sensitivity. On the other hand, adequate selectivity is ensured by judicious choice of target-specific antibodies. The timescale of these tests is determined by the time it takes for the sample to migrate to the test zone and is usually of the order of only a few minutes. In addition, even non-trained personnel, including the end users, can perform the test as only addition of a drop of sample in required. Finally, the transduction of analytical signal can be performed either visually for qualitative evaluation or using simple readers and low-cost commercial devices (scanners and smartphones) for quantitative measurements. Therefore, lateral flow immunoassays are particularly suitable for PoC in resource-limited environments being portable, affordable, robust, user-friendly, simple, sensitive, specific and rapid.

In this study, a colorimetric sandwich-type lateral flow immunoassay is developed for the detection of CEA in human serum. The sample/conjugation pad of the lateral flow strip is modified with gold nanoparticles (GNPs)-labeled anti-CEA conjugates which serve as probes and bind to the CEA target molecules in the sample; the complex is then captured at capture anti-CEA immobilized at the test line. In this work, the focus is on simplifying the construction, reducing the fabrication and operational cost of the biosensor and making it suitable for resource-limited POC settings. GNPS are used as functional signal reporters since their fabrication and their properties are extensively studied and well known.[29,30] The construction of the strip is greatly simplified as a single sample/conjugate pad is used. The amount of capture antibodies immobilized at the test line is reduced without compromising the sensitivity. Finally, the prerequisite for low-cost detection is fulfilled, since only a commercial inexpensive office scanner is required for quantification. The lateral flow immunoassay is validated in terms of linearity, limit of detection, matrix effects, reproducibility, accuracy and specificity.

2 Experimental

2.1 Materials and apparatus

All reagents used in this work are of analytical reagent grade. Ultrapure water (>18.2 MΩ cm^{-1}) is obtained using a Water Direct-Q® 3 UV Milli-Q water purification system (Merck Millipore, Burlington, MA, USA). Sucrose, polyethylene glycol (PEG) 20 000, polysorbate 20 (Tween 20), Triton X-114, polyvinylpyrrolidone (PVP), sodium hydroxide, boric acid, sodium borate decahydrate ($Na_2B_4O_7 \cdot 10H_2O$), potassium carbonate, carcinoembryonic antigen (CEA) (from human colon adenocarcinoma cell line), human blood serum (sterile & filtered) and hydrogen tetrachloroaurate(III)trihydrate ($HAuCl_4 \cdot 3H_2O$, ≥99.9%) are purchased from Sigma Aldrich (St. Louis, MO, USA). Ficoll F-400 (Mr 400 000) is from Sigma and Ficoll F-70 (Mr 70 000) is from Santa Cruz Biotechnology (Dallas, TX). Nitric acid 65%, potassium chloride, sodium chloride, potassium dihydrogen phosphate, disodium hydrogen phosphate and sodium citrate dihydrate ($Na_3C_6H_5O_7 \cdot 2H_2O$) are obtained from Chem-Lab (Zedelgem, Belgium). Bovine serum albumin (BSA) is from Thermo Scientific (Waltham, MA, USA), hydrochloric acid 30% is from Merck (Darmstadt, Germany) and sodium dodecyl sulfate (SDS) is from Honeywell Fluka (Charlotte, NC, USA). Cancer antigen 125 (from human ascites fluid adenocarcinoma) and cancer antigen 19-9 (from Human Metastatic Liver Carcinoma) are purchased from Medix Biochemica (Espoo, Finland).

The antibodies utilized as biorecognition elements are the monoclonal anti-h CEA 5909 SP-5 (as reporter antibody conjugated to GNPs), the anti-h CEA 5910 SPTN-5 (as capture antibody immobilized at the test line) and are purchased from Medix Biochemica (Espoo, Finland). The polyclonal goat anti-Mouse IgG (IgG AP124 Gt X Ms) serves as the capture antibody at the control line and is purchased from Merck (Darmstadt, Germany). The stock antibody solutions are diluted with a 20 mM phosphate buffer saline (PBS) (pH 7.4) before dispensing at the detection and control lines.

Standard CEA solutions are prepared in running buffer (50 mM PBS, 0.5% (w/v) Tween-20, 1% (w/v) BSA, 5% (w/v) sucrose, 0.6% (w/v) PEG), obtaining different analyte concentrations: 0.625, 1.25, 2.5, 5, 10, 20, 40, 80, 160, 320, 640 and 1280 ng mL^{-1}.

Syringe filters with a pore diameter of 0.20 μm are provided by Macherey-Nagel (Dueren, Germany). All the materials used for the fabrication of the immunosensor pad are purchased from Whatman Cytiva (Little Chalfont, Buckinghamshire, UK): nitrocellulose membranes Immunopore FP (5 μm, 25 mm × 50 m, 140–200 s/4 cm) and Immunopore RP (8 μm, 25 mm × 50 m, 90–150 s/4 cm) as the detection pads, STANDARD 17 bound glass fiber (34.5 s/4 cm, 22 mm × 50 m) as the sample/conjugate pad and chromatography paper 3 mm CHR (as the absorbent pad).

A Shimadzu UV-1800 (Kyoto, Japan) spectrophotometer is used to obtain the UV-vis absorption spectra of GNPs. The stirrer and the centrifuge are from Witeg (Wertheim, Germany). A semi-automatic sample dispenser (Camag Linomat 5, Muttenz, Switzerland) is used to spray the antibody solutions onto the nitrocellulose membrane in the form of bands to form the test and control lines. A HP Deskjet 2720 all-in-one printer-scanner (Palo Alto, CA, USA) is utilized to capture the images of the strips and Inkscape Version 1.2 is employed for image analysis. For RIA, a RIA kit (hCEA [I-125] IRMA, Institute of Isotopes Co Ltd, Budapest, Hungary) and a γ-counter (Genesys Gamma 1, Lablogic Systems Ltd, Sheffield, UK) are used in accordance with the manufacturers' instructions.

2.2 Methods

2.2.1 Synthesis of GNPs. GNPs are fabricated following a modification of the Turkevich method (Scheme S1, ESI†), which is based on the reduction of chloroauric acid ($HAuCl_4$) at 100 °C with sodium citrate.[31] 140 mL of a 0.25 mM $HAuCl_4$ aqueous solution is prepared in a 250 mL Erlenmeyer flask. The flask is placed on a magnetic hotplate stirrer and is covered with a watch glass to avoid contamination and evaporation of the solvent during the preparation. The solution is brought to a rolling boil while vigorously stirred, then 14 mL of 38.8 mM sodium citrate aqueous solution is rapidly added. Gradually, the color of the solution changes from pale yellow to deep wine red, suggesting the formation of the colloidal GNPs. The suspension is boiled under stirring for an additional 10 min, with the synthesis being complete when no further color change is observed. Thereafter, the solution is cooled down to room temperature with continuous stirring for another 15 min. The obtained colloid is passed through a 0.20 μm syringe filter and stored in dark bottles at 4 °C until further use. The synthesized GNPs are characterized by UV-Vis spectroscopy which reveals an absorption maximum at 520 nm (Fig. S1, ESI†) indicating an average particle size of 14 nm;[31] the average GNPs size did not differ by more than ±8% in three batches of GNPs synthesized in the course of this work. The solution can be stored for at least two months without precipitation. All glassware utilized in these preparations is thoroughly cleaned using freshly prepared aqua regia, rinsed with copious amounts of ultrapure H_2O and air-dried prior to use.

2.2.2 Preparation of the GNPs-labelled anti-CEA conjugate probes. For the preparation of GNPs-labelled anti-CEA conjugates, the reporter anti-h CEA 5909 SP-5 is conjugated to the GNPs through conventional passive adsorption following the method of Baryeh with slight modifications (Scheme S2, ESI†).[32] First, 6 mL of the GNPs solution is centrifuged at 12.400 rpm for 15 min. The supernatant is removed and the GNPs are resuspended in Milli-Q water whose pH has been previously adjusted to 9 with 0.2 M K_2CO_3 solution, resulting in 1.2 mL of 5-fold concentrated GNPs. 48 μg of anti-h CEA 5909 SP-5 antibody is pipetted into the GNPs solution (*i.e.* 40 μg of antibody per mL of GNP solution) and the mixture is initially vortexed and then gently shaken at 220 rpm at room temperature for 2 hours. The solution is then incubated at 4 °C overnight. To block the residual sites of the GNPs, 10% (w/v) BSA solution in 20 mM PBS (pH 7.4) is added dropwise to a final concentration of 1% (w/v) and the gentle shaking at 220 rpm is continued for 1 hour at room temperature. Next, the GNPs-labelled anti-CEA conjugates are washed three times with 20 mM PBS (pH 7.4) to ensure that unbound antibodies are removed; the conjugates are separated from the solution *via* centrifugation at 12.400 rpm for 15 min and re-suspended in the same volume of 1% (w/v) BSA solution in 20 mM PBS. Finally, the conjugates are re-suspended in 1.2 mL of resolvation buffer (20 mM PBS (pH 7.4) containing 5% BSA (w/v), 10% sucrose (w/v) and 0.25% (w/v) Tween-20). The GNPs-labelled anti-CEA conjugate probes are incubated in the refrigerator at 4 °C for 3 weeks before use.

2.2.3 Immobilization of reagents on the strip. The sample/conjugate pad is modified by pipetting 5 μL of the GNPs-labelled anti-CEA conjugates solution on the pad and left to air-dry.

The test and control lines of the strip are formed as follows. First, the capture anti-h CEA 5910 SPTN-5 and the IgG AP124 Gt X Ms antibodies are diluted in 20 mM PBS (pH 7.4) to final concentrations of 0.125 mg mL^{-1} and 0.25 mg mL^{-1}, respectively. Then, the capture anti-h CEA 5910 SPTN-5 solution is dispensed onto the nitrocellulose membrane using the semi-automatic sample dispenser at a flow rate of 2.86 μL cm^{-1} to form the test line. The IgG AP124 Gt X Ms antibodies solution is dispensed in the same manner at a distance of 0.6 cm downstream of the test line to form the control line. Therefore, 0.125 μg of anti-h-CEA 5910 and 0.25 μg of the IgG AP124 Gt X Ms antibody are used for each strip. The detection pad is subsequently dried on a hotplate at 37 °C for 1 h.

2.2.4 Assembly of the immunosensor strip. The immunosensor strip consists of three functional components mounted on a thin and flexible polyester card for support: a glass fiber sample/conjugation pad; a nitrocellulose membrane which serves as the detection pad, and; a cellulose absorption pad for enhancing the capillary flow. The conjugate, detection and absorbent pads, with a length of 2.2 cm, 2.5 cm and 2.5 cm respectively, are laminated onto the plastic baking card using a non-porous double sided sticky tape, with an overlap of around 0.2 cm between them. This ensures the continuous and uninterrupted flow of liquid along the immunosensor. The strips are then cut 0.35 cm wide and stored in dry conditions at 4 °C for up to a week. A schematic of the strip with components, dimensions and immobilized reagents is illustrated in Fig. 1a.

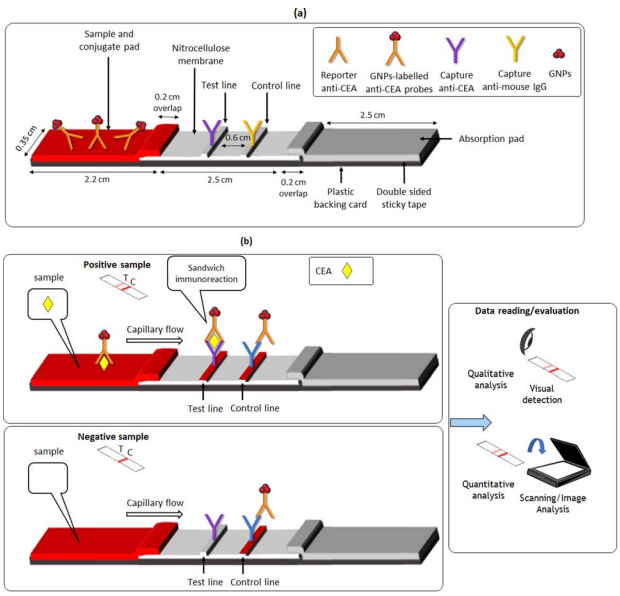

Fig. 1 (a) Schematic illustration of the construction of the lateral flow immunosensor developed for CEA detection showing the components, dimensions and immobilized reagents. (b) The principle of the sandwich-type immunoassay.

2.2.5 Lateral flow immunoassay and data evaluation. The principle of the lateral flow immunoassay for the detection of CEA is schematically illustrated in Fig. 1b. If the sample contains CEA (Fig. 1b, top), the target molecules bind with the immobilized GNPs-labelled anti-CEA conjugates at the sample/conjugate PAD and the complex is transported by solution flow to the nitrocellulose detection membrane. The complex is retained at the test line due to binding with the immobilized anti-CEA and the test line becomes red-colored (positive sample). If the sample placed at the sample/conjugate PAD does not contain CEA (Fig. 1b, bottom), the immobilized GNPs-labelled anti-CEA conjugates are transported by solution flow to the nitrocellulose detection membrane but are not retained at the test line which remains uncolored (negative sample). The intensity of the color at the test line can be further related to the CEA concentration in the sample for quantitative analysis. In both positive and negative samples, the excess immobilized GNPs-labelled anti-CEA conjugates are retained at the control line by the polyclonal goat anti-mouse IgG and the control line becomes red-colored, thus verifying that the test is valid.

The assay procedure consists of dispensing 50 μL of a standard CEA solution, sample or blank solution (running buffer) onto the sample/conjugate pad and allowing the liquid to flow. After 15 min, visual detection is performed for qualitative analysis. For quantitative analysis, the strips are scanned and the scanned images are imported into the open-access application Inkscape (**https://inkscape.org/**). The fluorescence filter is applied to enhance the contrast between the nitrocellulose background coloration and the test and control lines, thus increasing the signal-to-noise ratio. The color intensities of the test and control lines are determined with the Inkscape's Fill and Stroke tool using the Green component of the RGB color palette. To calculate the net signal due to CEA alone, the color intensity of the test line of each sample was subtracted from the color intensity of the test line of the blank sample.

3 Results and discussion

3.1 Selection of the experimental conditions

The overall performance of the lateral flow strips depends on the simultaneous interaction of several factors. The type of the nitrocellulose membrane, the formation of the control and test lines, the amount of antibody immobilized, the composition of the running buffer, the amount of reported antibody conjugated to the GNPs and the volume of GNPs-labelled-anti CEA conjugates solution used per test, were studied.

3.1.1 Nitrocellulose membrane type. The first line of optimization is choosing the type of nitrocellulose membrane which serves as the detection pad. Two membranes, Immunopore FP (5 μm pore diameter, 140–200 s/4 cm capillary flow rate) and Immunopore RP (8 μm pore diameter, 90–150 s/4 cm capillary flow rate) are assessed. In these membranes, the capillary flow rate determines the time available for the immunoreactions to occur at the test and control lines. The Immunopore RP membrane produces a lower intensity than the Immunopore FP at the test line and this is attributed to the larger pores of the Immunopore RP membrane, which allow for a faster flow rate and a reduced interaction time between CEA and the immobilized biorecognition elements (Fig. 2a). Therefore, the Immunopore FP nitrocellulose membrane is used for the following experiments.

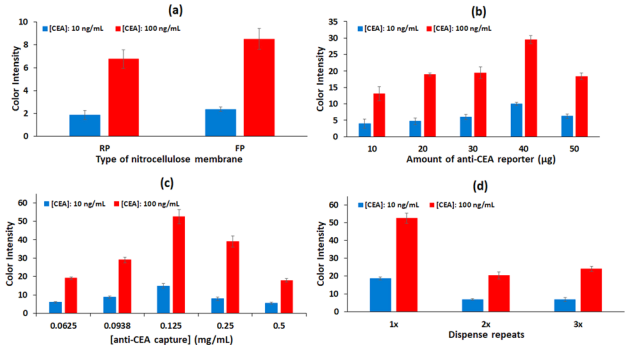

Fig. 2 Effect of different parameters on the performance of the lateral flow immunosensor for CEA detection (a) the type of the nitrocellulose membrane, (b) the amount of the anti-CEA per mL of the GNPs solution for the preparation of the GNPs-labelled anti-CEA conjugate probes, (c) the concentration of the capture anti-CEA solution immobilized at the test line, (d) the dispense cycles of the capture anti-CEA solution at the test line.

3.1.2 Antibody amount for the preparation the GNPs-labelled anti-CEA conjugated probes. The next parameter examined is the amount of reporter anti-CEA 5909 SP-5 conjugated with the GNPs. Different amounts of anti-CEA 5909 SP-5 (10, 20, 30, 40 and 50 μg) are added per mL of the 5-fold concentrated GNP solution for producing the GNPs-anti-CEA 5909 probe conjugates and the results are illustrated in Fig. 2b. The lowest signal intensity at the test line is observed using 10 μg of the reporter anti-CEA 5909 SP-5, since the amount of the antibody is not sufficient to achieve effective coverage of surface of the GNPs, leading to a decreased chance for a successful immunorecognition. As the amount of reporter anti-CEA 5909 SP-5 increases, so does the color intensity at the test line, with the more intense signal observed when 40 μg of the anti-CEA 5909 is used. At 50 μg of the reporter anti-CEA 5909 SP-5, a decrease in the color intensity is observed and this is likely the result of steric hindrance effects due to excessive loading of antibody moieties on the surface of the GNPs. Therefore, 40 μg of the reporter anti-CEA 5909 is chosen for the preparation of conjugates in the following experiments.

3.1.3 Volume of the GNPs-labelled anti-CEA conjugated probes applied at the sample/conjugate pad. The volume of the GNPs-anti CEA 5909 conjugate probes solution placed at the sample/conjugate pad is studied in the range 4–10 μL. 4 μL of the probes solution produces the weakest color intensity at the test line. At higher volumes (8 and 10 μL), the immunosensor produces a false positive result. The best results are observed at 5 and 6 μL with a satisfactory CEA signal at the test line combined with the absence of false positives. Finally, 5 μL is selected in the following experiments.

3.1.4 Effect of the concentration of the immobilized capture anti-CEA. The next parameters studied are the amount of the capture anti-CEA 5910 SPTN-5 es immobilized at the test

line. Two factors determined this amount: the concentration of the antibody solution used and the solution dispense times. Concentrations of 0.0625, 0.0938, 0.125, 0.25 and 0.5 mg mL^{-1} of anti-CEA 5910 SPTN-5 are tested (Fig. 2c). For lower concentrations of capture anti-CEA (0.0625 and 0.0938 mg mL^{-1}), there is not sufficient amount of capture antibodies at the test line, leading to a weaker signal. The strongest signal is observed for 0.125 mg mL^{-1} while 0.25 and 0.5 mg mL^{-1} lead to gradually weaker signal which is attributed to antibody overcrowding at the test line which either causes steric interferences or induces conformational changes of the immobilized antibodies. Then, the number of the dispense times of the 0.125 mg mL^{-1} anti-CEA 5910 Ab solution at the test line is assessed. The solution is dispensed 1×, 2× and 3× times at the test line of the nitrocellulose membrane allowing the lines to dry between each application. The most intense color is observed at 1× dispense times while multiple dispenses (2×, 3× times) result in signal reduction, probably due to spreading of the test line (Fig. 2d). Therefore, 1× dispense cycle and 0.125 mg mL^{-1} of the capture anti-CEA 5910 is selected.

3.1.5 Running buffer. The effect of the composition of the running buffer used to assist the flow along the immunosensor is studied next. The buffer is assessed with regard to the type of pH-adjusting salt used, the type of additional solutes added, as well as their concentrations. Initially, 50 mM (pH 7.4) PBS and sodium borate buffer solutions are compared. All solutions contain 5% (w/v) sucrose, 0.06% (w/v) Tween and 1% (w/v) BSA. PBS gives slightly better results, due to its slower flow rate which increased the time for the immunoreactions to occur and possibly because of its ability to enhance antibody stability *via* hydrogen bonding. Hence, PBS is chosen for the experiments that followed.

Next, different concentrations of sucrose (1%, 3%, 5% (w/v)) are examined. In addition to sucrose, the running buffer also contains 1% (w/v) BSA and 0.06% (w/v) Tween-20 in 50 mM PBS (pH 7.4). As previously reported, the addition of carbohydrates such as sucrose, lactose or trehalose, facilitates the release of the GNPs-labelled antibody conjugates from the conjugate pad.[33] This is confirmed in our experiments, since the immunosensor performs best with 5% (w/v) sucrose added, exhibiting higher color intensity at the test line (Fig. 3a). Higher concentrations of sucrose are not tested because they increase the viscosity and affect the flow of the running buffer.

At the same time, the concentration of polysorbate 20 (Tween-20) is evaluated. The role of Tween-20 in LFIAs is triple; it facilitates the re-solubilization of the GNPs–antibodies conjugate probes, it limits nonspecific interactions and it reduces the adsorption of the target analyte to the nitrocellulose membrane.[33] Solutions containing 0.1%, 0.25%, 0.5%, 0.75% and 1% (w/v) of Tween-20, along with 1% BSA and 5% sucrose in PBS 50 mM (pH 7.4) are compared and the best response is achieved using the 0.5% (w/v) Tween solution (Fig. 3b).

The next buffer component to be studied is BSA. BSA is often used in immunoassays to address non-specific binding and protein stability issues.[34] Solutions containing 0.2%, 0.5%, 1%, 2% and 5% (w/v) BSA along with 5% sucrose and 0.5% Tween in PBS 50 mM (pH 7.4) are compared. 1% (w/v) of BSA appears to provide the best signal for CEA (Fig. 3c); in contrast, higher BSA concentrations (2% and 5% (w/v)) result in false positive results. Therefore, the running buffer selected for further optimization contains 1% (w/v) BSA, 5% (w/v) sucrose and 0.5% (w/v) Tween in 50 mM PBS (pH 7.4).

The next component to be assessed is polyethylene glycol (PEG) 20 000. Macromolecular crowding agents such as PEG 20000 create a confining environment which enhances the efficiency of a successful immunoreaction between the target analyte and the biorecognition components. The agents can also increase the viscosity of the running buffer, decreasing the capillary flow rate and thus leading to improved sensitivity.[35] Solutions containing 0%, 0.6%, 1% and 5% (w/v) PEG along with 1% BSA, 5% (w/v) sucrose and 0.5% (w/v) Tween in PBS 50 mM (pH 7.4) are compared. The 0.6% (w/v) PEG concentration gives the highest signal at the test line and is thus chosen for the next experiments (Fig. 3d).

The effect of five more substances on the performance of the immunosensor's is evaluated. Different concentrations of Triton X-114, polyvinylpyrrolidone (PVP), sodium dodecyl sulfate (SDS), Ficoll-70 and Ficoll-400 are added to the buffer solution and the obtained results proved to be similar or worse than the aforementioned running buffer alone. Therefore, the buffer selected for further experiments contains 0.6% (w/v) PEG, 1% (w/v) BSA, 5% (w/v) sucrose and 0.5% (w/v) Tween-20 in 50 mM PBS (pH 7.4).

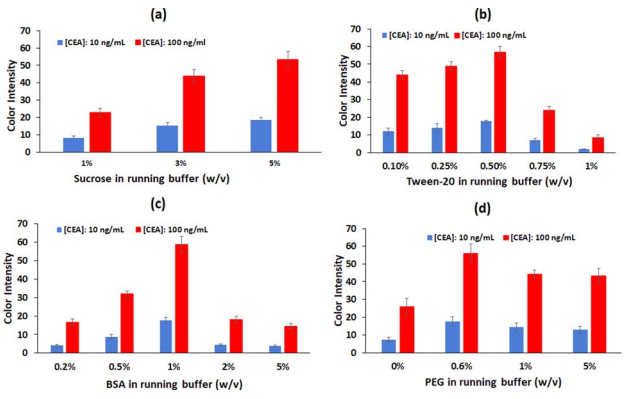

Fig. 3 The effect of the running buffer composition on the performance of the lateral flow immunosensor for CEA detection (a) content of sucrose, (b) content of Tween 20, (c) content of BSA, (d) content of PEG.

3.2 Metrological features of the immunosensor

3.2.1 Calibration of the immunosensor-limits of detection and quantification. CEA standard solutions with concentrations ranging from 0 to 1280 ng mL^{-1} (0, 1.25, 2.5, 5, 10, 20, 40, 80, 160, 320, 640, 1280 ng mL^{-1}) are prepared in the running buffer and are applied to the immunosensor under the selected conditions. Fig. 4a illustrates photos of the strips taken after the assays at different CEA concentrations. In the absence of CEA (blank sample), no color is observed in the test line indicating minimal non-specific interactions. On the other hand, the color intensity of the test line gradually increases with increasing

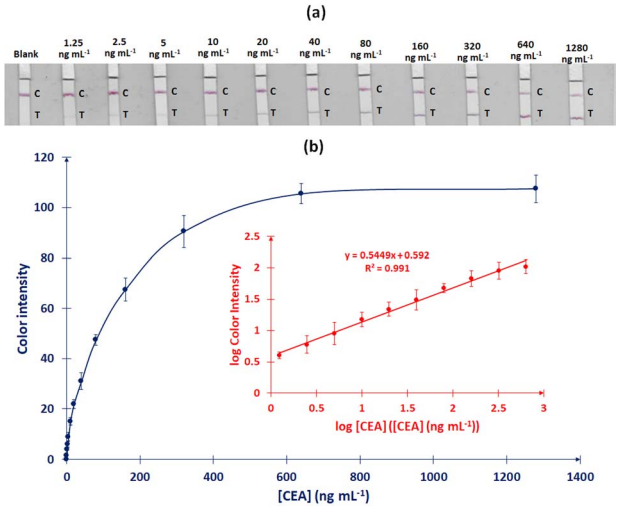

Fig. 4 (a) Photographs of the lateral flow strips after assays of different CEA concentrations (0–1280 ng mL^{-1}), (b) calibration graph for CEA determination (color intensity of the test line *vs.* CEA concentration), insert is the logarithmic calibration curve in the concentration range 1.25–640 ng mL^{-1} CEA. Each data point corresponds to the average color intensity of the test line from six replicate tests.

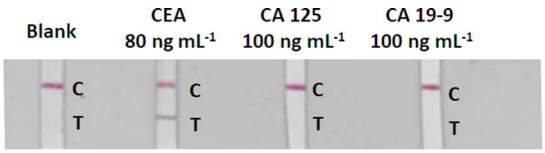

Fig. 5 Selectivity of the immunosensor. Blank and running buffer spiked with CEA, CA 125 and CA 19-9.

concentration of CEA. The calibration plot (net color intensity of the test line *vs.* the CEA concentration) is illustrated in Fig. 4b. The logarithmic calibration plot (logarithm of the net color intensity of the test line *vs.* the logarithm of the CEA concentration) exhibits a linear correlation over a wide concentration range (1.25 to 640 ng mL^{-1}) (inset in Fig. 5b). The instrumental limit of detection (LOD) is calculated as 0.45 ng mL^{-1} using the IUPAC definition (LOD = 3 SD_b/b, where SD_b is the standard deviation of the blank sample and b is the slope of the linear calibration curve using the low concentrations of the CEA standard solutions (1.25, 2.5, 5, 10 and 20 ng mL^{-1})). This value is consistent with the ng mL^{-1} level predicted as approximate instrumental LOD for conventional GNPs-based lateral flow tests using typical assay conditions.[36] The instrumental limit of quantification (LOQ) was set as the concentration of the more dilute standard in the calibration plot, *i.e.* 1.25 ng mL^{-1} (Fig. 4a). The visual LOD, defined as the CEA concentration that can be detected by the naked eye, is 0.63 ng mL^{-1}. Given that the threshold limit of CEA in clinical diagnosis is 5 ng mL^{-1}, the proposed is able to detect and quantify CEA in blood serum samples.

3.2.2 Assay specificity. To investigate the specificity of the developed immunosensor, two cancer specific markers which can coexist with CEA in patients' blood serum, are selected as potential interfering antigens. Running buffer is spiked with 80 ng mL^{-1} of CEA, 100 ng mL^{-1} of ovarian cancer-related tumor marker CA 125 and 100 ng mL^{-1} of carbohydrate antigen 19-9 (CA 19-9), respectively (Fig. 5). The absence of color in the test line in the presence of the CA125 or CA 19-9 antigens indicates no cross-reactivity and excellent specificity of the immunosensor.

3.2.3 Reproducibility-accuracy-matrix effects. Validation of the lateral flow immunosensor for clinical screening of CEA levels in serum samples involves study of the matrix effects, reproducibility and accuracy. For this purpose, a commercial human serum sample is used as the matrix. The sample is analyzed by RIA and the CEA concentration is found to be 1.8 ng mL^{-1}; all the quantitative measurements are corrected for the endogeneous CEA concentration. The blood serum sample is diluted 1 : 1 with a solution containing 1.2% (w/v) PEG, 2% (w/v) BSA, 10% (w/v) sucrose and 1% (w/v) Tween-20 in 100 mM PBS (pH 7.4), aliquots of the diluted solution are spiked with CEA to final concentrations of 2.5, 10, 40 και 160 ng mL^{-1} and the samples are analyzed in triplicate using the lateral flow immunosensor; scanned images of the assays are illustrated in Fig. S2 (ESI†).

To evaluate the matrix effect, the logarithmic calibration plot in the spiked sample is plotted and compared to the respective calibration plot using standards in running buffer (Fig. S3, ESI†). Statistical t tests demonstrate that the slopes and intercepts of the two calibration plots do not show statistically significant differences at the 95% confidence level; this suggests that the matrix effects are statistically insignificant and that the calibration plot using standards in running buffer can be used for the quantification of CEA in serum samples.

The recovery is calculated from the formula $R\% = C_c/C_{Sp}$ (where C_c is the CEA concentration calculated from the calibration curve in running buffer and C_{sp} is the concentration in the spiked sample). The results are summarized in Table 1 indicating recoveries between 87% and 115%. The reproducibility is expressed as the % relative standard deviation (% RSD)

Table 1 The recovery and reproducibility for a serum sample spiked with CEA using the lateral flow immunosensor

Level	Spiking in the spiked sample (ng mL^{-1})	Concentration detected (ng mL^{-1})	Recovery (%)	RSD (%)
1	2.5	2.36 ± 0.18	87–102	7.63
2	10	10.05 ± 1.01	90–111	10.05
3	40	44.74 ± 2.65	105–118	5.92
4	160	166.99 ± 16.66	94–115	9.98

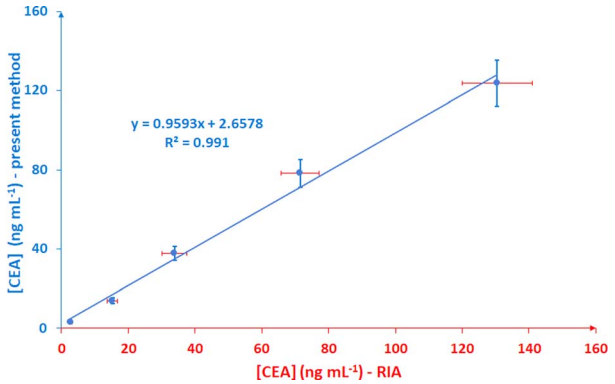

Fig. 6 Correlation between the present lateral flow immunoassay and RIA for CEA determination in spiked serum at 5 concentration levels.

of the triplicate measurements at each concentration level (Fig. S2, ESI†). As shown in Table 1, the % RSD values are between 7 and 11%.

Finally, the lateral flow immunoassay is compared with a radioimmunoassay (RIA) method which serves as a reference method. Human blood serum sample is diluted 1 : 1 with a solution containing 1.2% (w/v) PEG, 2% (w/v) BSA, 10% (w/v) sucrose and 1% (w/v) Tween in 100 mM PBS (pH 7.4), aliquots of the solution are spiked with CEA to final concentrations of 3, 15, 36, 72 και 120 ng mL^{-1} and the samples are analyzed in triplicate using the lateral flow immunosensor and RIA. As illustrated in Fig. 6, the two methods correlate well ($R^2 = 0.991$).

3.3 Comparison with existing immunosensors for CEA

Table S1 (ESI†) summarizes some characteristics of different lateral flow immunoassays for CEA reported in the literature.[37–46] The present lateral flow immunosensor is economical as it requires low amounts of immobilized antibodies, up to 6 times less compared to most of the existing methods (Table S1, ESI†). In two reports using a smaller amount of antibody at the test line, signal amplification techniques and a more complex protocol are used.[37,38]

The detection limit for CEA of the present immunosensor is 0.45 ng mL^{-1}. Some of the methods in Table S1 (ESI†) report lower LODs;[40,42] however, these methods use either fluorescence detection or reporter probes consisting of quantum dots (QDs), magnetic nanoparticles or combination of nanoparticles. However, fluorescence detectors require more complex instrumentation (namely an excitation source) and are more expensive while QD$_S$ and magnetic nanoparticles are more expensive to purchase and more difficult to synthesize and functionalize than GNPs. Therefore, these methods are more expensive and complex and do not lend themselves to applications in low-resource environments. On the other hand, considering that the cut-off value for CEA is 5 ng mL^{-1},[47,48] methods with LODs< 1 ng mL^{-1} are actually suitable for CEA detection within the clinically accepted range. Most often, the methods with extremely low detection limits have limited narrow linear dynamic range at higher concentrations necessitating dilution of some samples.[40,42] In contrast, the present immunosensor exhibits a wide linear dynamic range (1.25–640 ng mL^{-1}), 2 to 12 times wider than most literature reports (Table S1, ESI†).

Some previous applications are based on capturing images of the strips with smartphones;[38] however, this approach has some serious limitations as many unpredictable factors can contribute to the final coloration of the captured image.[49] On the other hand, optical readers commercially available[39,41,42,46] or made in-house[37,40,44] have been used for signal transduction but these are not suitable for low-resource settings as the former are expensive while the latter require laborious fabrication steps. In this work, we utilize a commercial-all-in one office printer-scanner, a low-cost device (<50 €) widely available in office and home settings which provides stable lighting conditions leading to reproducible results.

Another advantage of the present immunosensor is that it shows similar response to the running buffer and human serum samples so that calibration using standards prepared in the running buffer is sufficient for quantification purposes. Finally, the fabrication of the present strip is simpler as it makes use of only three pads as opposed to existing lateral flow assays that make use of four or more pads in the strip.

To assess whether the developed immunosensor is economically sustainable, the cost of the reagents per strip is calculated. The components that mainly determine the total cost of the device are the antibodies, the nitrocellulose membrane and the bound glass fiber pad. The total cost of materials at retail prices required to prepare one immunosensor for CEA detection amounts to ~0.19 € (Fig. S4, ESI†).

4 Conclusions

In this study, a lateral flow assay is developed for the detection of CEA in human serum. The lateral flow strip is low-cost (<0.20 €/per device), its fabrication is simplified compared to conventional strips, it makes use of low amounts of expensive reagents and a single drop of sample and offers a limit of detection of 0.45 ng mL^{-1} (which is well below the 5 ng mL^{-1} cut-off value for CEA) using only a low-cost office scanner. The assay is selective for CEA, is free from serum matrix effects, is accurate and reproducible. Therefore, the operational, fabrication and analytical features suggest that the lateral flow immunosensor is fit-for purpose for the detection and quantitation of CEA at the PoC or in low-resource environments.

Author contributions

Conceptualization, A. E., C. K. and V. P.; methodology, A. E. and V. P.; validation, V. P., I. T. and E. M.; investigation, V. P., I. T. and E. M.; data curation, V. P., I. T., A. E. and E. M.; writing—original draft preparation, I. T. and C. K.; writing—review and editing, A. E., C. K., V. P. I. T.; project administration, A. E.; funding acquisition, A. E.

Conflicts of interest

There are no conflicts to declare.

Acknowledgements

The research project was supported by the Hellenic Foundation for Research and Innovation (H. F. R. I.) under the "2nd Call for H. F. R. I. Research Projects to support Faculty Members & Researchers" (Project Number: 2956).

References

1 Cancer, WHO, **https://www.who.int/news-room/fact-sheets/detail/cancer**, accessed February 2024.
2 F. Bray, A. Jemal, N. Grey, J. Ferlay and D. Forman, Global cancer transitions according to the Human Development Index (2008–2030): a population-based study, *Lancet Oncol.*, 2012, **13**(8), 790–801.
3 M. Malvezzi, C. Santucci, P. Boffetta, G. Collatuzzo, F. Levi, C. La Vecchia and E. Negri, European cancer mortality predictions for the year 2023 with focus on lung cancer, *Ann. Oncol.*, 2023, **34**(4), 410–419.
4 A. Roberts and S. Gandhi, A concise review on potential cancer biomarkers and advanced manufacturing of smart platform-based biosensors for early-stage cancer diagnostics, *Biosens. Bioelectron.: X*, 2022, **11**, 100178.
5 M. Pal, T. Muinao, H. P. D. Boruah and N. Mahindroo, Current advances in prognostic and diagnostic biomarkers for solid cancers: Detection techniques and future challenges, *Biomed. Pharmacother.*, 2022, **146**, 112488.
6 L. Wu and X. Qu, Cancer biomarker detection: recent achievements and challenges, *Chem. Soc. Rev.*, 2015, **44**, 2963–2997.
7 C. Hall, L. Clarke, A. Pal, P. Buchwald, T. Eglinton, C. Wakeman and F. Frizelle, A Review of the Role of Carcinoembryonic Antigen in Clinical Practice, *Ann. Coloproctol.*, 2019, **35**(6), 294–305.
8 M. J. Duffy, Carcinoembryonic antigen as a marker for colorectal cancer: is it clinically useful?, *Clin. Chem.*, 2001, **47**(4), 624–630.
9 S. Hammarström, The carcinoembryonic antigen (CEA) family: structures, suggested functions and expression in normal and malignant tissues, *Semin. Cancer Biol.*, 1999, **9**, 67–81.
10 E. Ermiah, M. Eddfair, O. Abdulrahman, M. Elfagieh, A. Jebriel, M. Al-Sharif, M. Assidi and A. Buhmeida, Prognostic value of serum CEA and CA19-9 levels in pancreatic ductal adenocarcinoma, *Mol. Clin. Oncol.*, 2022, **17**(2), 126.
11 H. Mizuno, H. Miyake, H. Nagai, Y. Yoshioka, K. Shibata, S. Asai, J. Takamizawa and N. Yuasa, Optimal cutoff value of preoperative CEA and CA19-9 for prognostic significance in patients with stage II/III colon cancer, *Langenbeck's Arch. Surg.*, 2021, **406**, 1987–1997.
12 G. R. Nicol, M. Han, J. Kim, C. E. Birse, E. Brand, A. Nguyen, M. Mesri, W. FitzHugh, P. Kaminker, P. A. Moore, S. M. Ruben and T. He, Use of an Immunoaffinity-Mass Spectrometry-based Approach for the Quantification of Protein Biomarkers from Serum Samples of Lung Cancer Patients, *Mol. Cell. Proteomics*, 2008, **7**(10), 1974–1982.
13 R. Falzarano, V. Viggiani, S. Michienzi, F. Longo, S. Tudini, L. Frati and E. Anastasi, Evaluation of a CLEIA automated assay system for the detection of a panel of tumor markers, *Tumor Biol.*, 2013, **34**, 3093–3100.
14 S. Qu, J. Liu, J. Luo, Y. Huang, W. Shi, B. Wang and X. Cai, A rapid and highly sensitive portable chemiluminescent immunosensor of carcinoembryonic antigen based on immunomagnetic separation in human serum, *Anal. Chim. Acta*, 2013, **766**, 94–99.
15 X. Yang, Y. Guo and A. Wang, Luminol/antibody labeled gold nanoparticles for chemiluminescence immunoassay of carcinoembryonic antigen, *Anal. Chim. Acta*, 2010, **666**(1–2), 91–96.
16 J. Y. Hou, T. C. Liu, G. F. Lin, Z. X. Li, L. P. Zou, M. Li and Y. S. Wu, Development of an immunomagnetic bead-based time-resolved fluorescence immunoassay for rapid determination of levels of carcinoembryonic antigen in human serum, *Anal. Chim. Acta*, 2012, **734**, 93–98.
17 Z. Tan, L. Cao, Y. Yang, Q. Yan, Q. Liu, W. Zhang, P. Zhao, Y. Li and D. Zhang, Amperometric immunoassay for the carcinoembryonic antigen by using a peroxidase mimic consisting of palladium nanospheres functionalized with glutathione-capped gold nanoparticles on graphene oxide, *Mikrochim. Acta*, 2019, **186**(11), 693.
18 H. Chon, S. Lee, S. Wook Son, C. Hwan Oh and J. Choo, Highly Sensitive Immunoassay of Lung Cancer Marker Carcinoembryonic Antigen Using Surface-Enhanced Raman Scattering of Hollow Gold Nanospheres, *Anal. Chem.*, 2009, **81**(8), 3029–3034.
19 X. Gu, Z. She, T. Ma, S. Tian and H. B. Kraatz, Electrochemical Detection of Carcinoembryonic Antigen, *Biosens. Bioelectron.*, 2018, **102**, 610–616.
20 Y. Wang, G. Zhao, Y. Zhang, X. Pang, W. Cao, B. Du and Q. Wei, Sandwich-Type Electrochemical Immunosensor for CEA Detection Based on Ag/MoS2@Fe3O4 and an Analogous ELISA Method with Total Internal Reflection Microscopy, *Sens. Actuators, B*, 2018, **266**, 561–569.
21 Y. Wang, Y. Wang, D. Wu, H. Ma, Y. Zhang, D. Fan, X. Pang, B. Du and Q. Wei, Label-Free Electrochemical Immunosensor Based on Flower-like Ag/MoS2/RGO Nanocomposites for Ultrasensitive Detection of Carcinoembryonic Antigen, *Sens. Actuators, B*, 2018, **255**, 125–132.
22 T. Špringer and J. Homola, Biofunctionalized Gold Nanoparticles for SPR-Biosensor-Based Detection of CEA in Blood Plasma, *Anal. Bioanal. Chem.*, 2012, **404**, 2869–2875.
23 R. Li, F. Feng, Z. Z. Chen, Y. F. Bai, F. F. Guo, F. Y. Wu and G. Zhou, Sensitive Detection of Carcinoembryonic Antigen Using Surface Plasmon Resonance Biosensor with Gold Nanoparticles Signal Amplification, *Talanta*, 2015, **140**, 143–149.
24 A. Sena-Torralba, R. Álvarez-Diduk, C. Parolo, A. Piper and A. Merkoçi, Toward Next Generation Lateral Flow Assays: Integration of Nanomaterials, *Chem. Rev.*, 2022, **122**(18), 14881–14910.
25 T. Mahmoudi, M. de la Guardia and B. Baradaran, Lateral flow assays towards point-of-care cancer detection: A

review of current progress and future trends, *TrAC, Trends Anal. Chem.*, 2020, **125**, 115842.
26 K. Omidfar, F. Riahi and S. Kashanian, Lateral Flow Assay: A Summary of Recent Progress for Improving Assay Performance, *Biosensors*, 2023, **13**(9), 837.
27 M. K. Dey, M. Iftesum, R. Devireddy and M. R. Gartia, New technologies and reagents in lateral flow assay (LFA) designs for enhancing accuracy and sensitivity, *Anal. Methods*, 2023, **23**, 4351–4376.
28 E. Gumus, H. Bingol and E. Zor, Lateral flow assays for detection of disease biomarkers, *J. Pharm. Biomed. Anal.*, 2023, **225**, 115206.
29 I. Ielo, G. Rando, F. Giacobello, S. Sfameni, A. Castellano, M. Galletta, D. Drommi, G. Rosace and M. R. Plutino, Synthesis, Chemical–Physical Characterization, and Biomedical Applications of Functional Gold Nanoparticles: A Review, *Molecules*, 2021, **26**, 5823.
30 M. I. Anik, N. Mahmud, A. Al Masud and Md. M. Hasan, Gold nanoparticles (GNPs) in biomedical and clinical applications: A review, *Nano Sel.*, 2022, **3**, 792.
31 J. Dong, P. L. Carpinone, G. Pyrgiotakis, P. Demokritou and B. M. Moudgil, Synthesis of Precision Gold Nanoparticles Using Turkevich Method, *Kona*, 2020, **37**, 224–232.
32 K. Baryeh, *Development of quantitative lateral flow strip biosensors for the detection of cancer biomarkers, Doctoral Dissertation, Department of Chemistry and Biochemistry*, North Dakota State University of Agriculture and Applied Science, 2019, **https://library.ndsu.edu/ir/bitstream/handle/10365/29881/Baryeh_ndsu_0157D_12268.pdf?sequence=1&isAllowed=y**, accessed in February 2024.
33 M. Kaur and E. Eltzov, Optimizing Effective Parameters to Enhance the Sensitivity of Vertical Flow Assay for Detection of *Escherichia coli*, *Biosensors*, 2022, **12**(2), 63.
34 A. Sukumaran, T. Thomas, R. Thomas, R. E. Thomas, J. K. Paul and D. M. Vasudevan, Development and Troubleshooting in Lateral Flow Immunochromatography Assays, *Indian J. Clin. Biochem.*, 2021, **36**(2), 208–212.
35 N. M. Christopoulou, D. Kalogianni and T. Christopoulos, Macromolecular crowding agents enhance the sensitivity of lateral flow immunoassays, *Biosens. Bioelectron.*, 2022, **218**, 114737.
36 B. N. Khlebtsov, R. S. Tumskiy, A. M. Burov, T. E. Pylaev and N. G. Khlebtsov, Quantifying the Numbers of Gold Nanoparticles in the Test Zone of Lateral Flow Immunoassay Strips, *ACS Appl. Nano Mater.*, 2019, **2**(8), 5020–5028.
37 T. Mahmoudi, M. Pourhassan-Moghaddam, B. Shirdel, B. Baradaran, E. Morales-Narváez and H. Golmohammadi, On-Site Detection of Carcinoembryonic Antigen in Human Serum, *Biosensors*, 2021, **11**(10), 392.
38 T. Mahmoudi, B. Shirdel, B. Mansoori and B. Baradaran, Dual sensitivity enhancement in gold nanoparticles-based lateral flow immunoassay for visual detection of carcinoembryonic antigen, *Anal. Sci. Adv.*, 2020, **1**, 161–172.
39 Q. Zeng, X. Mao, H. Xu, S. Wang and G. Liu, Quantitate Immunochromatographic Strip Biosensor for the Detection of Carcinoembryonic Antigen Tumour Biomarker in Human Plasma, *Am. J. Biomed. Sci.*, 2009, **1**(1), 70–79.
40 K. Xiao, K. Wang, W. Qin, Y. Hou, W. Lu, H. Xu, Y. Wo and D. Cui, Use of quantum dot beads-labeled monoclonal antibody to improve the sensitivity of a quantitative and simultaneous immunochromatographic assay for neuron specific enolase and carcinoembryonic antigen, *Talanta*, 2017, **164**, 463–469.
41 Z. Chen, R. Liang, X. Guo, J. Liang, Q. Deng, M. Li, T. An, T. Liu and Y. Wu, Simultaneous quantitation of cytokeratin-19 fragment and carcinoembryonic antigen in human serum *via* quantum dot-doped nanoparticles, *Biosens. Bioelectron.*, 2017, **91**, 60–65.
42 W. Lu, K. Wang, K. Xiao, W. Qin, Y. Hou, H. Xu, X. Yan, Y. Chen, D. Cui and J. He, Dual immunomagnetic nanobeads-based lateral flow test strip for simultaneous quantitative detection of carcinoembryonic antigen and neuron specific enolase, *Sci. Rep.*, 2017, **7**, 42414.
43 F. Liu, H. Zhang, Z. Wu, H. Dong, L. Zhou, D. Yang, Y. Ge, C. Jia, H. Liu, Q. Jin, J. Zhao, Q. Zhang and H. Mao, Highly sensitive and selective lateral flow immunoassay based on magnetic nanoparticles for quantitative detection of carcinoembryonic antigen, *Talanta*, 2016, **161**, 205–210.
44 W. Qin, K. Wang, K. Xiao, Y. Hou, W. Lu, H. Xu, Y. Wo and S. Feng, D. Cui Carcinoembryonic antigen detection with "handing"-controlled fluorescence spectroscopy using a color matrix for point-of-care applications, *Biosens. Bioelectron.*, 2017, **90**, 508–515.
45 Y. Wu, W. Peng, Q. Zhao, J. Piao, B. Zhang, X. Wu, H. Wang, Z. Shi, X. Gong and J. Chang, Immune fluorescence test strips based on quantum dots for rapid and quantitative detection of carcino-embryonic antigen, *Chin. Chem. Lett.*, 2017, **28**(9), 1881–1884.
46 B. Zhang, W. Ma, F. Li, W. Gao, Q. Zhao, W. Peng, J. Piao, X. Wu, H. Wang, X. Gong and J. Chang, Fluorescence quenching-based signal amplification on immunochromatography test strips for dual-mode sensing of two biomarkers of breast cancer, *Nanoscale*, 2017, **9**, 18711–18722.
47 L. Gan, S. Ren, M. Lang, G. Li, F. Fang, L. Chen, Y. Liu, R. Han, K. Zhu and T. Song, Predictive value of preoperative serum AFP, CEA, and CA19-9 levels in patients with single small hepatocellular carcinoma: retrospective study, *J. Hepatocell. Carcinoma*, 2022, **9**, 799–810.
48 H. Zhang, C. Li, F. Hu, X. Zhang, Y. Shen, Y. Chen and F. Li, Auxiliary diagnostic value of tumor biomarkers in pleural fluid for lung cancer-associated malignant pleural effusion, *Respir. Res.*, 2020, **21**, 1–7.
49 S. Soares, G. M. Fernandes and F. R. P. Rocha, Smartphone-based digital images in analytical chemistry: Why, when, and how to use, *TrAC, Trends Anal. Chem.*, 2023, **168**, 117284.